Acta Neurochirurgica (2019) 161:695–706
https://doi.org/10.1007/s00701-018-03778-0

ORIGINAL ARTICLE - PITUITARIES

Application of indocyanine green fluorescence endoscopic system in transsphenoidal surgery for pituitary tumors

Kosaku Amano[1] · Yasuo Aihara[1] · Shunsuke Tsuzuki[1] · Yoshikazu Okada[1] · Takakazu Kawamata[1]

Received: 30 April 2018 / Accepted: 18 December 2018 / Published online: 14 February 2019

Abstract

Background For the precise removal of pituitary tumors, preserving the surrounding normal structures, we need real-time intraoperative information on tumor location, margins, and surrounding structures. The aim of this study was to evaluate the benefits of a new intraoperative real-time imaging modality using indocyanine green (ICG) fluorescence through an endoscopic system during transsphenoidal surgery (TSS) for pituitary tumors.

Methods Between August 2013 and October 2014, 20 patients with pituitary and parasellar region tumors underwent TSS using the ICG fluorescence endoscopic system. We used a peripheral vein bolus dose of 6.25 mg/injection of ICG, started with a time counter, and examined how each tissue type increased and decreased in fluorescence through time.

Results A total of 33 investigations were performed for 20 patients: 9 had growth hormone secreting adenomas, 6 non-functioning pituitary adenomas, 3 Rathke's cleft cysts, 1 meningioma, and 1 pituicytoma. After the injection of ICG, the intensity of fluorescence of tumor and normal tissues under near-infrared light showed clear differences. We could differentiate tumor margins from adjacent normal tissues and define clearly the surrounding normal structures using the different fluorescent intensities time changes and tissue-specific fluorescence patterns.

Conclusions The ICG endoscopic system is simple, user-friendly, quick, cost-effective, and reliable. The method offered real-time information during TSS to delimit pituitary and parasellar region tumor tissue from surrounding normal structures. This method can contribute to the improvement of total removal rates of tumors, reduction of complications after TSS, saving surgical time, and preserving endocrinological functions.

Keywords Endoscope · Indocyanine green fluorescence · Pituitary tumor · Real-time information · Transsphenoidal surgery · Tumor visualization

This article is part of the Topical Collection on *Pituitaries*

✉ Kosaku Amano
kamano@twmu.ac.jp

Yasuo Aihara
yaihara@nij.twmu.ac.jp

Shunsuke Tsuzuki
st09212005@yahoo.co.jp

Yoshikazu Okada
yokada@twmu.ac.jp

Takakazu Kawamata
tkawamata@twmu.ac.jp

[1] Department of Neurosurgery, Tokyo Women's Medical University, 8-1 Kawada-cho, Shinjuku-ku, Tokyo 162-8666, Japan

Abbreviations

CS	Cavernous sinus
CT	Computed tomography
GHoma	Growth hormone-producing pituitary adenoma
ICG	Indocyanine green
ICS	Intercavernous sinus
MRI	Magnetic resonance image
NFoma	Non-functioning pituitary adenoma
RCC	Rathke's cleft cysts
TSS	Transsphenoidal surgery
T1WIGd	T1-weighted image with gadolinium enhancement

Introduction

During pituitary tumor removal, we have to define tumor margins to surrounding structures for precise removal without

unnecessary injury and functional damage. However, intraoperative decision-making and tissue identification are strongly dependent on the surgical experience of the operating surgeon. In pituitary surgery in general, we decide the surgical plan upon the detailed preoperative MRI and differentiate tumor tissue from surrounding structures at surgery according to its macroscopic properties, based predominantly on subjective evaluation of tissue color, consistency (soft, hard, fibrous, or viscous), capillary reperfusion, and so on. Objective methods—intraoperative rapid diagnosis—have been used clinically, but are technically demanding, require additional time and human resources, and are not absolutely reliable. Therefore, there is still a need for a simple, reliable tissue and structure identification method that can be applied during surgery, not interfering with observation and manipulation, and provide us truly real-time information.

Indocyanine green (ICG) is a near-infrared fluorescent tricarbocyanine dye, approved by the Food and Drug Administration in 1959 for cardiocirculatory and liver function diagnostic use. Since then for more than half a century, this method was available to and developed in many branches of medicine, such as ophthalmology, plastic surgery, and abdominal surgery [18–20, 24]. In digestive surgery, Noura et al. reported that the ICGFE was useful for the detection of lymph node metastases in lower rectal cancer [33].

In the neurosurgical field, ICG is used to visualize blood vessels using fluorescence and has the advantages for real-time intraoperative visualization of cerebral perfusion. This noninvasive method is simple, safe, cost-effective, easily repeatable, and convenient and provides the surgeon instantaneous information as a tool supporting intraoperative decision-making to produce pictures reflecting blood flow. A microscope integrated ICG videoangiography (ICG-VAG) has been introduced for intraoperative cerebral blood flow monitoring during vascular surgery for aneurysms, arterial bypasses, arteriovenous malformations or arteriovenous fistulas, and Moyamoya disease [8, 12, 22, 25, 29, 31, 32, 35, 36, 38, 43]. Recently, ICG-VAG application has been widely extended to a greater variety of neurosurgical diseases including tumors, such as cavernous angiomas, hemangioblastomas, meningiomas, metastatic tumors, gliomas, and adenomas [7, 10–12, 23, 37, 39, 41, 42]. These reports evaluated the usefulness of the method not only for vascular diseases but also for brain and spinal canal tumors. However, most of those reports assessed the vascularity of the tumor itself and its surrounding structures, but not specifically for tumor delineation and characterization.

On the other hand, the endoscope is an absolutely necessary tool in TSS to visualize wide areas, particularly in the parasellar region and many reports have already demonstrated its application in TSS [3, 4, 6, 9, 17, 28]. Though TSS has some specific complications [1, 5] and maneuverability during this surgery is restricted due to anatomical and technical factors, we tried to overcome them by developing appropriate surgical instruments [21]. Therefore, we are now able to remove pituitary tumors more aggressively in endoscopic TSS with panoramic view and high-resolution image. The ICG fluorescence endoscope system was an innovative tool in which ICG angiographic images could be observed through the endoscope in real-time.

Only four experimental and clinical studies applying an ICG endoscopic system in brain tumor removal have been conducted so far. Litvack et al. first reported the usefulness of ICG fluorescence endoscope (ICGFE) for pituitary adenoma removal as a pilot study [27]. They applied ICG in pituitary adenomas with a customized endoscopy and concluded that identifying the tumor by the difference of fluorescence intensity enabled safe and complete removal. We (Tsuzuki et al.) reported that ICGFE was able to visualize vessels, tumor masses, and surrounding structures even in an intraventricular environment and was useful for detection of the tumor in endoscopic biopsy [40]. Hide et al. also reported the application of ICGFE for an intracavernous dermoid cyst removal as a case report [15] and the clear confirmation of anatomical landmarks, especially vessels [16]. Thus, ICGFE should be considered a promising tool with great potential for further application in tumor removal.

In this report, we designed a more detailed attempt for visual differentiation of pituitary and parasellar region tumors from surrounding structures by using the ICG fluorescence endoscopic system in TSS and tried to expand its practical application further on as a new intraoperative real-time imaging modality.

Materials and methods

Between August 2013 and October 2014, 20 patients with pituitary and parasellar region tumors underwent TSS supported by navigation using an ICG fluorescence endoscopic system at our institute. The characteristics of the patients and final pathological diagnoses are shown in Table 1. ICG has been proven to be safe and is routinely applied in our everyday surgical work. Therefore, ICG was included in the informed consent for every patient preoperatively mentioning that it provided additional possibilities for tumor detection and the disadvantage of extending additionally surgical time. The recommended dose of ICG dye is 0.2 to 0.5 mg/kg, and the maximum daily dose should not exceed 5 mg/kg. We used a dose of 6.25 or 12.5 mg/injection of ICG (DAIICHI SANKYO, Co. Ltd.) into a peripheral vein given as a bolus. After the bolus injection of ICG intravenously, the dye bonds to large plasma proteins within 1–2 s and remains intravascular in the conditions of normal vascular permeability. The dye is excreted exclusively by the liver with a plasma half-life of 150 s. It demonstrates maximum fluorescence in human blood at an excitation wavelength of 820 nm. This spectral shift is due to the binding of the dye to plasma proteins.

Table 1 Characteristics of the 20 patients and result of ICG examination

Case	Age/ gender	Tumor history	Dose and frequency of ICG injection	Tumor fluorescence[a]
1	50/M	FSH+, LH+ adenoma	6.25 mg × 1, 12.5 mg × 1	+
2	67/F	silent ACTH+ adenoma	6.25 mg × 1	+
3	47/F	silent GH+ adenoma	6.25 mg × 1	+
4	54/F	GH+ adenoma	6.25 mg × 2	+
5	73/F	FSH+, LH+ adenoma	6.25 mg × 2	+
6	51/F	GH+ adenoma	6.25 mg × 3	+
7	58/F	Null-cell adenoma	6.25 mg × 3	+
8	30/F	Rathke's cleft cyst	6.25 mg × 2	−
9	52/F	GH+ adenoma	6.25 mg × 1	+
10	35/M	Null-cell adenoma	6.25 mg × 1	+
11	69/M	GH+, PRL+ adenoma	6.25 mg × 2	+
12	42/M	Pituicytoma	6.25 mg × 1	−
13	47/F	GH+, TSH+ adenoma	6.25 mg × 2	+
14	43/F	Rathke's cleft cyst	6.25 mg × 1	−
15	73/M	GH+, PRL+ adenoma	6.25 mg × 1	+
16	59/M	GH+, PRL+ adenoma	6.25 mg × 1	+
17	68/F	Atypical meningioma	6.25 mg × 1	+
18	42/F	GH+ adenoma	6.25 mg × 2	+
19	22/M	Rathke's cleft cyst	6.25 mg × 2	−
20	32/M	GH+ adenoma	6.25 mg × 2	+

FSH follicle-stimulating hormone, *LH* luteinizing hormone, *ACTH* adrenocorticotropic hormone, *GH* growth hormone, *PRL* prolactin, *TSH* thyroid-stimulating hormone

[a] Tumor fluorescence stronger than the normal gland during 6 to 8 min after injection of ICG

The ICG technique visualization was performed using the following light equipment: KARL STORZ Photodynamic Diagnosis (PDD) D-light P system, Image 1 HUBTM HD camera control unit, IMAGE 1 H3-Z FI 3-Chip ICG FULL HD camera head (1920 × 1080 pixels), and a straight forward ICG telescope (0°, diameter 5.8 mm/length 19 cm). After the bolus dye injection, followed with a 10-cm^3 normal saline bolus, we started a time count and examined the points in time for each tissue of fluorescence appearance, its intensity increase, intensity peak, decrease, and disappearance. Observing the illuminated field, we switched the light source from white to near-infrared light by a foot switch and examined the change of ICG tissue fluorescence. The dynamics of the image could be observed on the monitor in real time and quantifications of fluorescence intensity change were visually confirmed and approved by the operator and assistant independently. After the initial or additional fluorescence examination, tumor mass margins were delineated and the extent of removal decided. Tumor removal was performed under standard endoscopic illumination. The excised fluorescent lesions were examined histologically and the histopathological findings were correlated to the ICG endoscopic findings. All patients in this study underwent a thorough pre- and postoperative endocrine workup to confirm the diagnosis and pituitary function.

Results

A total of 33 investigations were performed for 20 patients (Three times ICG injections during the same surgery were done in 2 cases, three times in 9 cases, and once in 9 cases.); 9 tumors were growth hormone-producing pituitary adenomas (GHomas), 6 non-functioning pituitary adenomas (NFomas), 3 Rathke's cleft cysts (RCCs), 1 meningioma, and 1 pituicytoma (Table 1). There were neither complications during and after surgery that can be

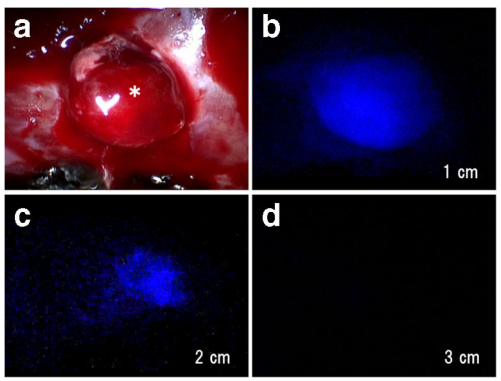

Fig. 1 The appearance of a pituitary adenoma under white light (**a**) and the same field of view under near-infrared light after injection of ICG, at a distance of 1 cm (**b**), 2 cm (**c**), and 3 cm (**d**)

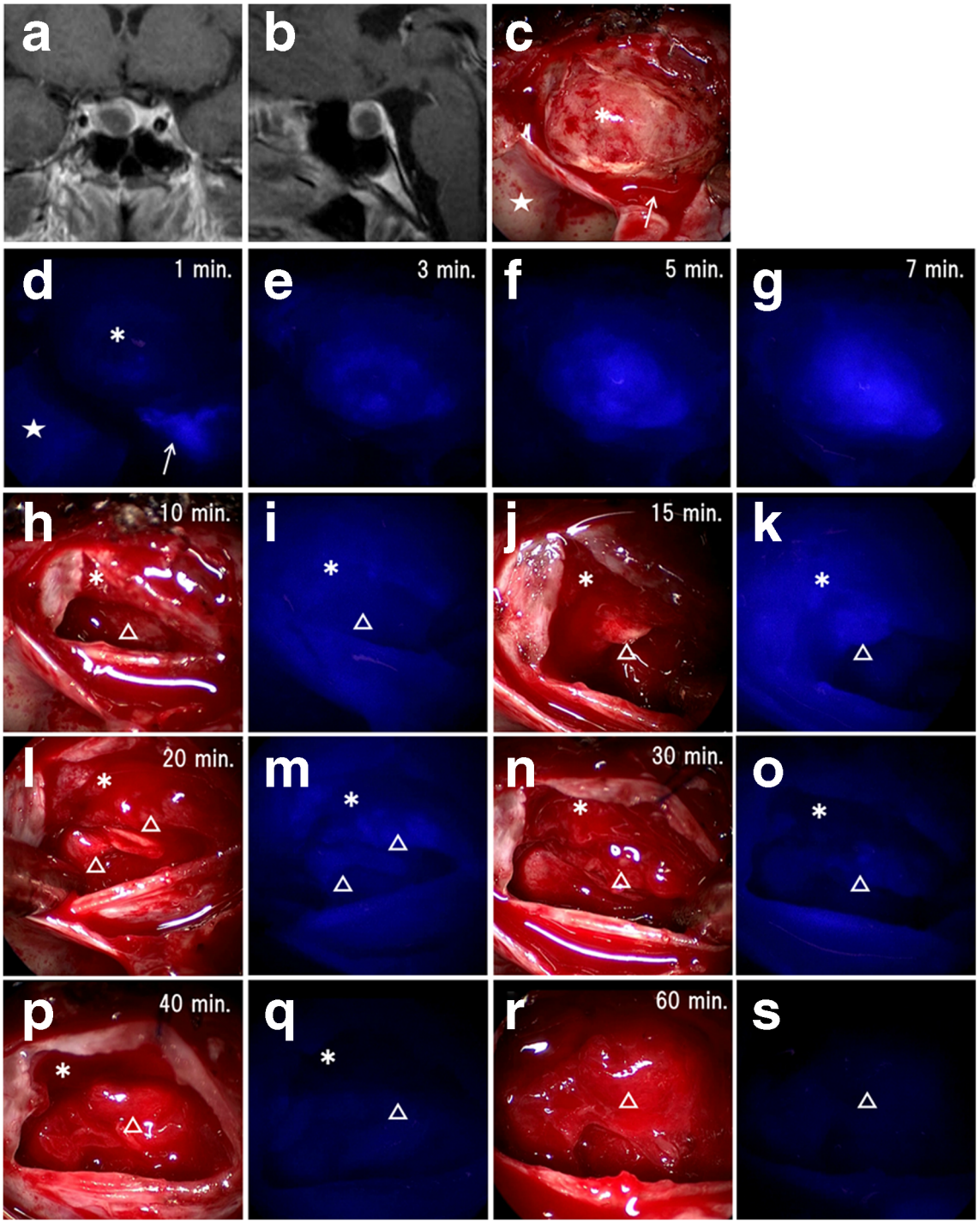

Fig. 2 Illustrative images obtained in a 50-year-old man with a NFoma. Preoperative coronal MRI, T1WIGd (**a**) and sagittal MRI, T1WIGd (**b**). The images demonstrate the appearance of the opened sellar floor, adenoma (asterisk), internal carotid prominence (star), and oozing blood (arrow) under white light **(c)** and the same field of view under near-infrared light 1 min (**d**), 3 min (**e**), 5 min (**f**), and 7 min (**g**) after injection of ICG. The internal carotid artery (star) and oozing blood (arrow) are identified 1 min after the injection of ICG (**d**). Note that fluorescence intensity from the adenoma is getting gradually stronger since the 1st to the 7th minute after the ICG injection (**d**–**g**). By removing the tumor, fluorescence intensity from the adenoma became gradually weaker from the 8th to the 15th minute after ICG injection (**h**–**k**). On the other hand, the fluorescence intensity from the normal gland became gradually stronger from the 10th to the 40th minute and then again weaker from the 40th to the 60th minute after ICG injection (**h**–**s**)

attributed to the ICG injection nor other general complications related to the surgery itself.

Fluorescence intensity of tumor also depended on the distance between the object and lens (as shown in Fig. 1), so each

observation and comparison of fluorescent intensities was performed from the same distance. The usual distance from the object was approximately 1 cm and we considered acceptable a range of up to 2 cm.

Non-functioning pituitary adenomas

Fluorescent intensity of these adenomas gradually increased from 1 to 7 min after the ICG injection and then gradually decreased until the 15th minute as shown on Fig. 2c–g; meanwhile, the normal gland also gradually became fluorescent starting about 10 to 20 min after injection and gradually less fluorescent from the 30th to the 60th minute, as in Fig. 2h–s. The tumor was best visualized about 7 min after injection and the normal gland was better visualized than the tumor after 15 min onward (Fig. 9). Therefore, we could distinguish the tumor clearly from the normal gland within 15 min of observation after injection. The technique demonstrated that the tumor was removed precisely, the normal gland was preserved completely, and as a result patient's endocrinological functions were improved after surgery.

Internal carotid arteries

The location of internal carotid arteries (ICA) was identified before opening the sella turcica by the carotid prominence appearance as in Fig. 2d.

Sphenopalatine artery

The location and direction of sphenopalatine arteries under the nasoseptal mucosa were identified 1 min after the ICG injection as in Fig. 3a, b.

Cavernous sinus and intercavernous sinus

Figure 4 illustrates a GHoma invading the cavernous sinus (CS). The venous flow of CS and intercavernous sinus (ICS) were identified 2 min after the ICG injection (Fig. 4c); therefore, dural incision design permitted to minimize venous bleeding (Fig. 4d). On the other hand, Fig. 5 shows another GHoma invading the CS, but the venous flow of the CS and ICS were not identified at 2 min after the ICG injection (Fig. 5c). In this case, the tumor that invaded and packed CS was identified 7 min after the ICG injection (Fig. 5e). The CS wall was opened to remove the CS tumor portion, but there was no venous bleeding (Fig. 5f).

Posterior lobe of pituitary gland

The posterior lobe of pituitary gland was differentiated from the anterior around 2 min after the ICG injection, as demonstrated in Fig. 3c–e. The well-vascularized anterior pituitary gland has been fluorescing after the 3rd minute; however, the posterior lobe was best visualized between the 2nd and 5th minutes after injection as shown on Fig. 9. With this approach, we could distinguish the posterior lobe from the anterior about 2 to 3 min after injection.

Rathke's cleft cyst

The normal gland compressed by the cyst content was pale and its fluorescence intensity was weak 15 min after the ICG injection as shown in Fig. 6c, d. After removal of the cyst content, the decompressed normal gland showed better blood flow and its fluorescence intensity became strong 15 min after the ICG injection, as in Fig. 6e, f.

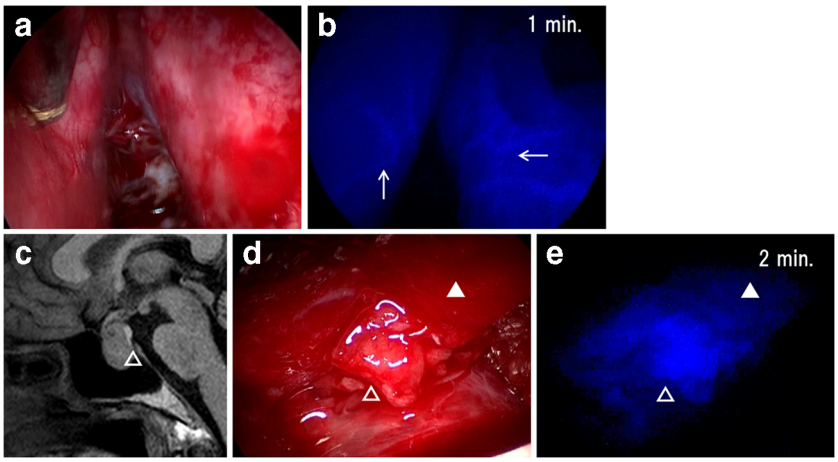

Fig. 3 Visualization of the sphenopalatine artery in the nasal cavity under white light (**a**) and the same field of view under near-infrared light 1 min after injection of ICG (**b**). Preoperative sagittal MRI, T1WI (**c**) demonstrating the posterior lobe as a high-intensity area. ICG fluorescence in the same case demonstrates different density between the anterior and posterior lobes of the normal gland. **d** The appearance of the normal gland, anterior lobe (white triangle), and posterior lobe (triangle); after tumor removal under white light and the same field of view under near-infrared light 3 min after injection of ICG (**e**) demonstrating the contrast between anterior and posterior lobes

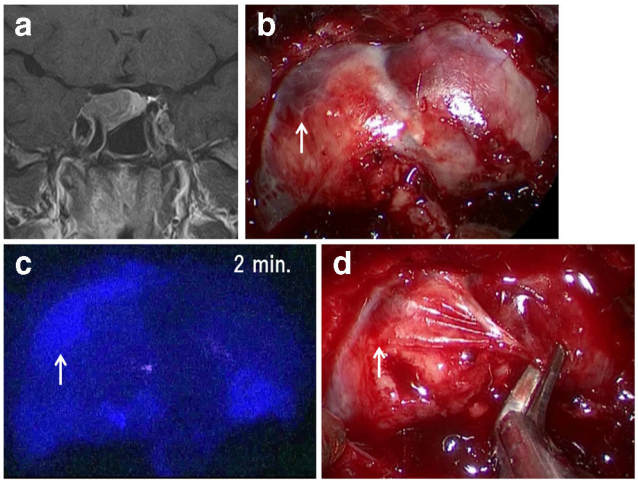

Fig. 4 Illustrative images obtained in a 59-year-old man with a GH-producing pituitary adenoma. Preoperative coronal MRI, T1WIGd (**a**), cavernous and intercavernous sinuses under white light (**b**) and the same field of view under near-infrared light 2 min after ICG injection (**c**), indicating patency of the right cavernous sinus (arrow). The dura is incised at the margin of the cavernous sinus (arrow) to avoid venous bleeding (**d**)

Growth hormone-producing adenoma

During tumor removal, the cleavage between residual tumor and revealed normal gland was clearly identified at 6 min after the ICG injection as seen in Fig. 7c, d. After total removal of the tumor, the decompressed normal gland became gradually brighter 8 min after the ICG injection as in Fig. 7e, f. The tumor was removed totally, and the postsurgical endocrinological examinations demonstrated to be clear of Cortina consensus (75 g OGTT nadir, 0.14 ng/ml; IGF-1, 178 ng/ml) and no GH deficiency (GHRP-2, 39.83 ng/ml).

Pituicytoma

The pituicytoma, a very rare tumor in the pituitary region, did not show fluorescence 7 min after the ICG injection as in Fig. 8, whereas a pituitary adenoma usually became highly fluorescent at the same time-sequence after injection. This phenomenon can warn the surgeon that the tumor was not an adenoma, but another type of lesion.

ICG fluorescence intensity changes of tumor and normal tissues in time-sequence

After the injection of ICG into a peripheral vein, fluorescent intensity of tumor and normal tissues under near-infrared light changed with time, as shown in Fig. 9. The fluorescence curves were determined through averaging of patients data.

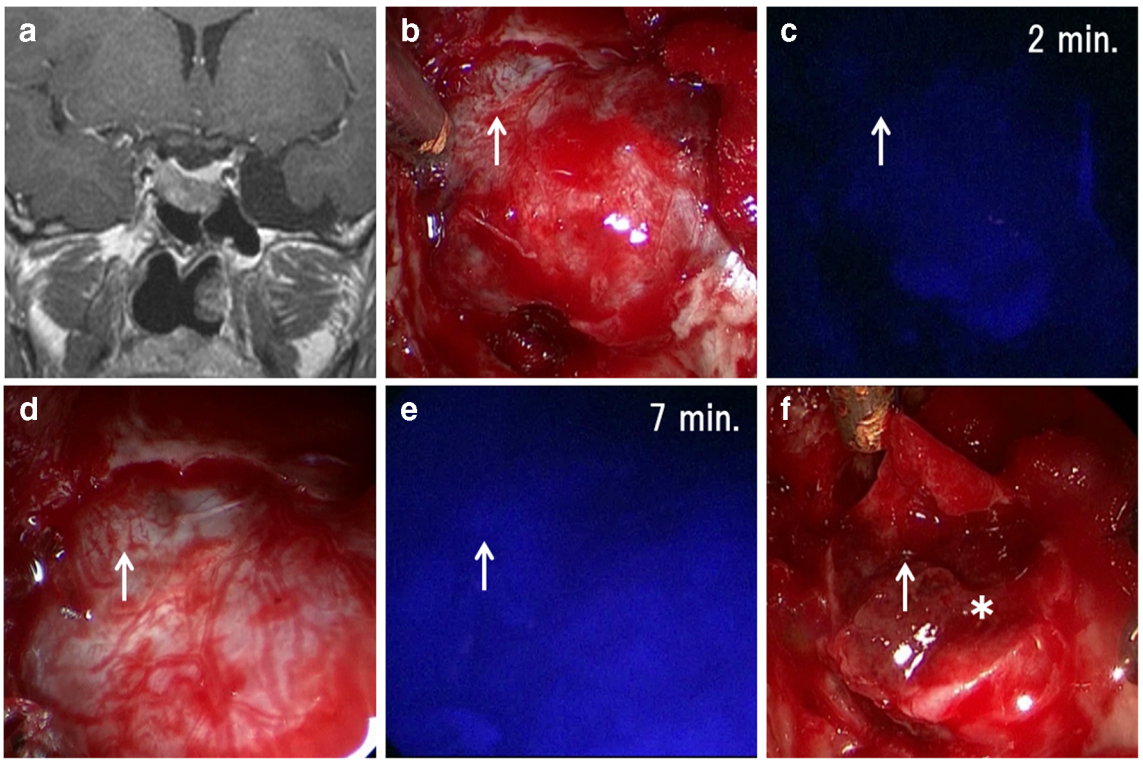

Fig. 5 Illustrative images obtained in a 42-year-old woman with a GH-producing pituitary adenoma. Preoperative coronal MRI, T1WIGd (**a**), the cavernous (arrow), and intercavernous sinuses under white light (**b**) and the same field of view under near-infrared light 2 min after ICG injection (**c**), indicating no patency of the cavernous sinus (arrow). **d** The close-up view of the cavernous sinus (arrow) under white light and the same field of view under near-infrared light 7 min after ICG injection, showing the cavernous sinus filled with tumor (arrow) (**e**). The dura was incised over the cavernous sinus (arrow) but there was no venous bleeding because of tumor packing (asterisk) (**f**)

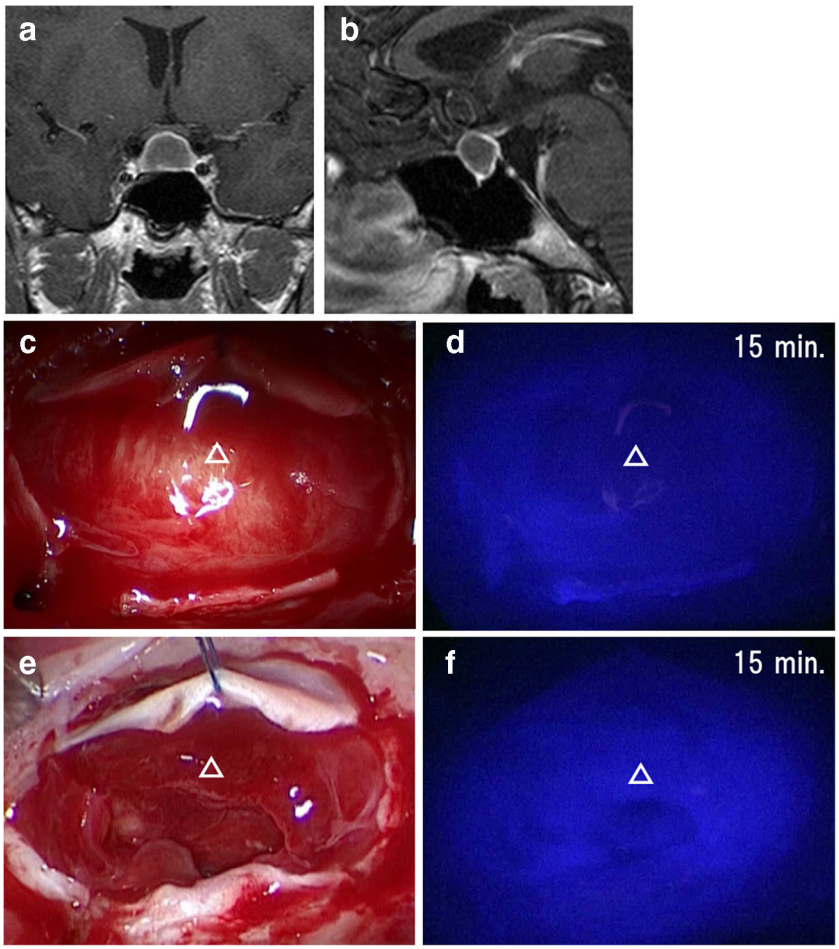

Fig. 6 Illustrative images obtained in a 22-year-old man with a Rathke's cleft cyst. Preoperative coronal MRI, T1WIGd (**a**) and sagittal MRI, T1WIGd (**b**). **c** The appearance of a thin/ischemic normal gland (triangle) prior to removing the cyst content under white light and the same field of view under near-infrared light 15 min after injection of ICG (**d**). **e** The same field of vascular normal gland (triangle) after removing the cyst content under white light and the same field of view under near-infrared light 15 min after injection of ICG (**f**). The vascularized normal gland (**f**) showed stronger ICG fluorescence than the thin/ischemic normal gland (**d**)

We could observe and differentiate tumors from other normal tissues using these changes of fluorescence intensities in relation to time and differences of fluorescence patterns.

Discussion

The ICGFE is an optical instrument with enhanced properties. In this study, we took the ICGFE one step further and focused on the time changes of ICG fluorescence intensity of tumors and normal tissues under near-infrared light as shown in Fig. 9. Although in previous reports, the use of ICG in brain tumors was mainly evaluating their vascularity, our study focused on the temporal characteristics of dye distribution. This permitted the definition of tumor margins in relation to the normal pituitary and the parasellar region structures, which are not much more vascular than surrounding normal structures. Normal surrounding structure identification remains a cardinal goal in TSS, especially in cases of anatomical variations or displacement due to the tumor [46].

Figure 9 presents time-sequence diagrams of the ICG fluorescent intensity changes of tumor and normal tissues under near-infrared light. We focused our attention not only on the appearance and increase of fluorescence intensity but also on its decay. To shorten the time of fluorescence fading, the amount of bolus ICG was fixed at 6.75 mg, a smaller amount when compared with the standard ICG-VAG using 12.5 or 25 mg. As a result, the fluorescence intensity showed temporal differences for each tissue compared to the tumor. For example, for the period 1–7 min after the ICG bolus, the pituitary adenoma was more fluorescent than the normal anterior pituitary lobe, but that became the opposite from the 8th minute onward. After tumor removal, the normal gland improved its vascular perfusion due to decompression and had higher fluorescence intensity 15 min after the bolus (Fig. 6).

We have sometimes difficulties to differentiate between a tumor and normal gland after removing tissues located at a cleavage between them. We intended to remove small residual tumor parts completely in microadenomas and resect only the tumor without injuring the compressed and distorted, often very thin normal gland to preserve or improve pituitary functions in macroadenomas. Therefore, we routinely performed dynamic contrast MRI preoperatively to reveal any significant differences in appearance between pituitary tumors and the normal pituitary gland. There were some reports that the dynamic study was useful for this purpose and the normal gland was enhanced

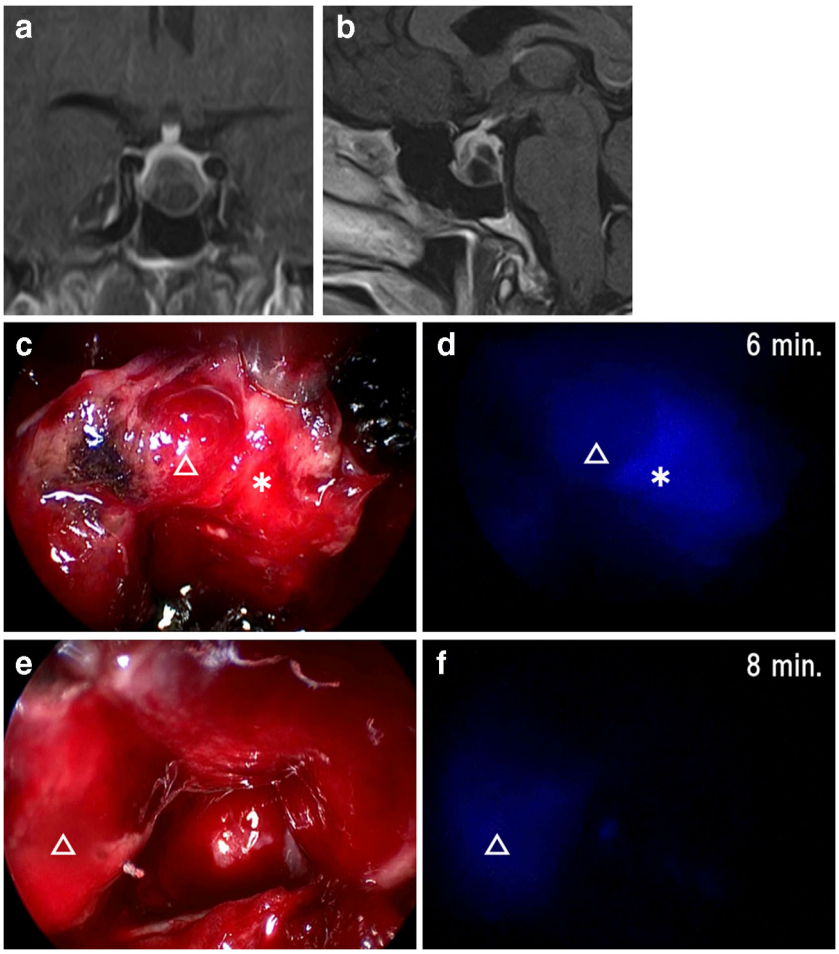

Fig. 7 Illustrative images obtained in a 51-year-old woman with a GH- producing pituitary adenoma. Preoperative coronal MRI, T1WIGd (**a**) and sagittal MRI, T1WIGd (**b**). **c** The appearance of the normal gland (triangle) and adenoma (asterisk) in the process of tumor removal under white light and the same field of view under near-infrared light 6 min after ICG injection (**d**), the last showing clear cleavage between the normal gland and the adenoma. After removal of the tumor (**e**), there is no more tumor fluorescence, but the normal gland (triangle) became fluorescent 8 min after ICG injection (**f**)

at an earlier phase than the adenoma [30]. There is discrepancy between the early fluorescence of pituitary adenoma seen through the ICGFE and the findings of dynamic MRI. A pituitary adenoma is reached by the contrast at the speed of the arterial flow [14, 44] and pituitary microadenomas demonstrates early enhancement with dynamic CT [2]. We can speculate that a pituitary adenoma is in fact enhanced earlier than the normal gland during the dynamic MRI study, but that is not detected because it enhances too early and too briefly and eventually because of its hypo-vascularity.

Fujisawa et al. reported that the posterior pituitary lobe showed high signal intensity on T1WI.

These MRI findings were useful to determine the location of posterior lobe [13, 26]. The posterior lobe was identified as a white and soft tissue during surgery, so sometimes it was difficult to differentiate it from the pituitary adenoma especially in GHomas, which are also white and soft. The ICGFE enables us to distinguish the anterior and posterior lobe of the pituitary gland as shown in Fig. 3e, f.

Information on vascular structures is very important during endoscopic TSS. We must be aware of the location of the internal carotid arteries (ICA) to prevent surgical complications, often serious and sometimes fatal. As shown in Fig. 2d, the ICA was identified by the carotid prominence. As shown in Fig. 3b, sphenopalatine arteries were also identified clearly 1 min after the ICG injection. The detection of sphenopalatine arteries within the nasoseptal mucosa is necessary for preserving vascularity that later will be needed for a nasoseptal flap and preventing significant nasal bleeding intra- and postoperatively. The location of sphenopalatine artery was variable and it can be difficult to identify even using Doppler. Before ICG introduction, we became aware of the sphenopalatine artery when it was already injured. Not only arteries but also visualization of the venous channels around the pituitary, such as the cavernous (CS) and intercavernous sinuses (ICS), was also important to prevent bleeding while opening the sellar floor dura and removing tumor tissue invading the sinuses. We aggressively removed tumors in the cavernous sinus, especially in functioning adenomas, to improve the functional remission rate. Through this procedure, it is very important to reduce the amount of venous bleeding. Though it was difficult to estimate the degree of tumor invasion to the CS and the patency of the CS and ICS using preoperative MRI, the ICG endoscopic evaluation provided useful information about the patency of the venous system for the area of intended removal. In this way, we could decide where and how long to open the cavernous sinuses wall (Figs. 4 and 5).

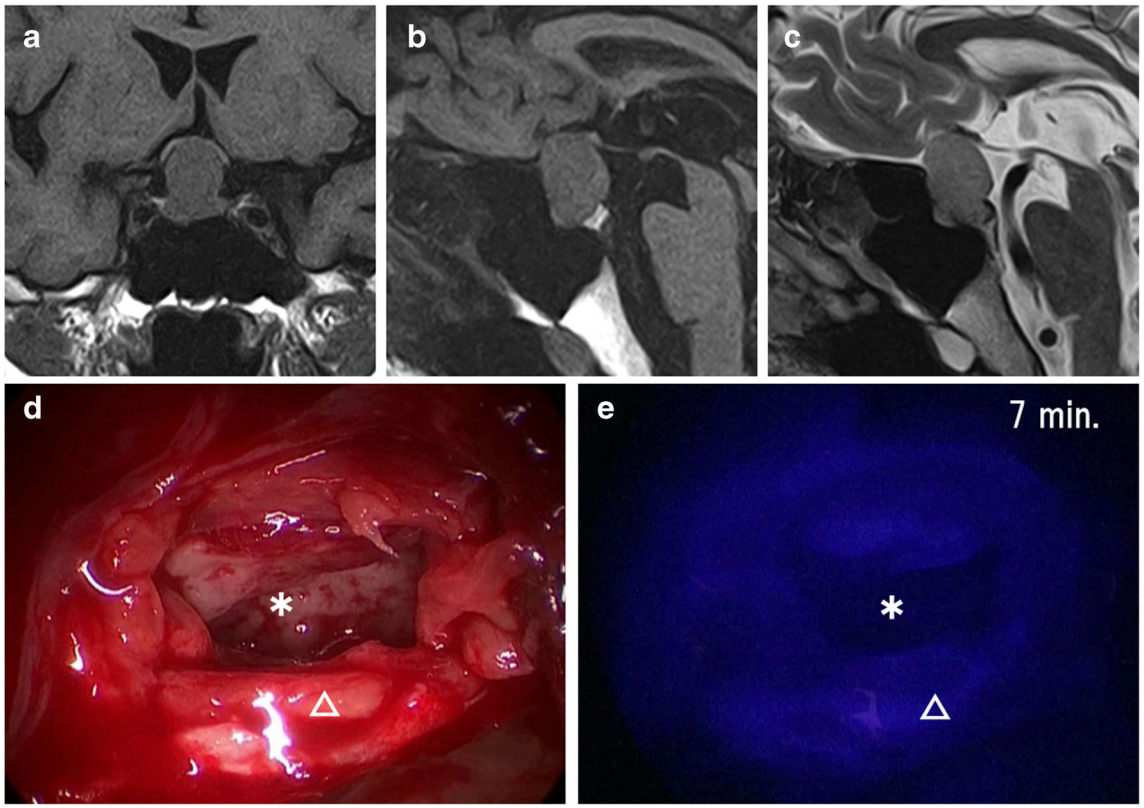

Fig. 8 Illustrative images obtained in a 42-year-old man with a pituicytoma. Preoperative coronal MRI, T1WI (**a**), sagittal MRI, T1WI (**b**), and T2WI (**c**). **d** The appearance of the normal gland (triangle) and tumor (asterisk) in the process of tumor removal under white light. The same field of view under near-infrared light 7 min after ICG injection (**e**) showed relative absence of fluorescence of the tumor compared with pituitary adenomas

Routinely, to identify structures and distinguish normal from abnormal tissues, the surgeon analyses the MRIs in detail and correlates them with intraoperative observations: location, relationships, tissue color, soft or hard consistence, and so on. However, these determinations are quite subjective and might differ according to the surgeon's experience and other factors. Additionally, to obtain objective information about the tumor, we use intraoperative frozen sections. However, the intraoperative diagnosis takes a relatively long time compared to the progress of tumor removal and at times provides only general pathological information. "Rapid" growth hormone measurement during TSS is also useful as intraoperative information for GHoma removal. However, it can be used only in GHomas and is not a true real-time information. Otani et al. reported that its sensitivity and specificity were not so high—59.2 and 59.5% [34].

ICGFE with its 5.8 mm diameter is larger than the normal high definition endoscope (2.7 and 4 mm). Its thickness sometimes obstructs the movement of surgical instruments and devices. The absence of angled scope lenses and irrigation sheath equipment were the other inconveniences of the ICGFE. Angled endoscopes (30°, 45°, and 70°) are absolutely necessary for removal of far lateral and superior tumor parts

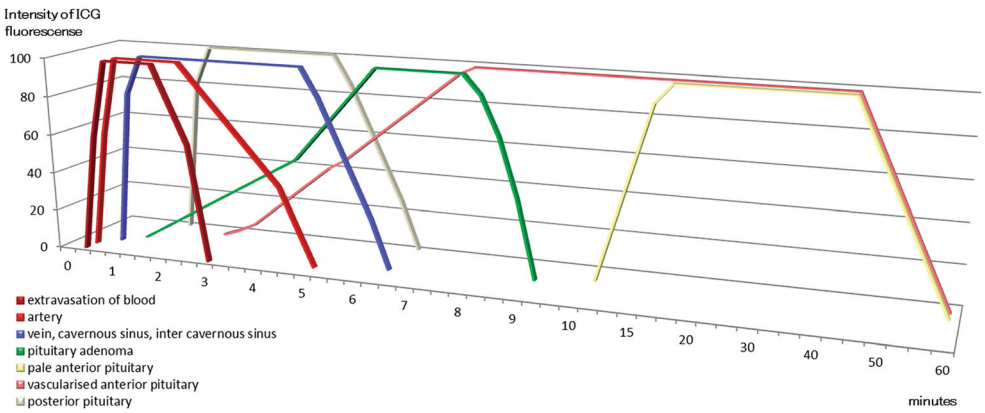

Fig. 9 **a**–**f** Time-sequence diagrams of ICG fluorescence intensity changes of a pituitary adenoma and normal tissues

and an irrigation sheath is very convenient to clean up the tip of the endoscope during surgery. As a result of these technical limitations, if a critical intraoperative situation demands, the endoscope should be exchanged for the common white light endoscope during tumor removal. We expect a technical solution to these problems to be found in the near future.

When using fluorescence as a surgical adjunct, we need to think about the kinetics of dye extravasation, vascular clearance, photobleaching, and tissue light penetration. What is more, there is a possibility that ICGFE infrared light emission can affect normal brain arteries. White emboli formation was observed on the inner side of vessel walls within seconds after starting light exposure in photodynamic therapy for malignant tumors [45]. Though there are no reports that ICG under near-infrared light affects vessels so far, near-infrared light should be used as briefly as possible considering this possibility.

As shown in Fig. 8, a pituicytoma, because of ICGFE, we could realize that the tumor was not an adenoma, but something that was not predicted before surgery. This was an advantage of ICGFE that, although not conclusive at the moment, could be developed for intraoperative diagnostic purposes in future.

Currently, the ICGFE cannot yet completely replace the present endoscopic standards. One of the most important limitations of imaging through the ICGFE is its non-quantitative type of information. The intraoperative evaluation of fluorescence intensity in this study was consistently evaluated subjectively by the operator's and assistant's naked eye on the monitor. Hide et al. demonstrated quantitative data using photoshop postoperatively [16], but imaging through the ICGFE will be considered more reliable if quantitative analysis can be performed intraoperatively in real time. The potential of the ICGFE in TSS must be based on further investigations from which the relationship to increased or diminished perfusion should also be evaluated, eventually providing the possibility to distinguish the type and degree of tumor malignancy. That can complement intraoperative frozen section studies for tumor type diagnosis. As a next step, further experience and consideration of fluorescence intensity of each structure will be required and quantitative data analysis should be introduced. There is a possibility that microadenomas in Cushing disease that are sometimes difficult to be identified on preoperative MRI and be detected during surgery. If tumor fluorescence proves useful for tumor detection, it may improve surgical decision-making and gross total removal rate, decrease surgical time, reduce new endocrinopathy and complication rates and thereby lead to better clinical results.

Conclusions

Intraoperative optical identification of pituitary and parasellar region tumors and differentiation of the tumor from surrounding normal structures using ICG fluorescence endoscopic system is a simple, feasible, quick, cost-effective, safe, non-invasive, and reliable method of offering real-time information during TSS. This system may lead to the improvement of the total removal rate of pituitary tumors, reducing complications after TSS and saving operation time, and preservation of endocrinological functions.

Acknowledgements We would like to thank Kostadin L. Karagiozov, MD, PhD, for his review of this manuscript and Ichiro Fujisawa, radiologist, for the advice on MRI of pituitary adenoma.

Compliance with ethical standards

Conflict of interest The authors declare that they have no competing interests.

Ethical approval All procedures performed in studies involving human participants were in accordance with the ethical standards of the institutional and/or national research committee and with the 1964 Helsinki declaration and its later amendments or comparable ethical standards.

Informed consent Informed consent was obtained from all individual participants included in the study.

Publisher's note Springer Nature remains neutral with regard to jurisdictional claims in published maps and institutional affiliations.

References

1. Amano K, Hori T, Kawamata T, Okada Y (2016) Repair and prevention of cerebrospinal fluid leakage in transsphenoidal surgery: a sphenoid sinus mucosa technique. Neurosurg Rev 39:123–131; discussion 131. https://doi.org/10.1007/s10143-015-0667-6
2. Bonneville JF, Cattin F, Gorczyca W, Hardy J (1993) Pituitary microadenomas: early enhancement with dynamic CT—implications of arterial blood supply and potential importance. Radiology 187:857–861. https://doi.org/10.1148/radiology.187.3.8497646
3. Campbell PG, Teo KS, Worthley SG, Kearney MT, Tarique A, Natarajan A, Zaman AG (2009) Non-invasive assessment of saphenous vein graft patency in asymptomatic patients. Br J Radiol 82:291–295. https://doi.org/10.1259/bjr/19829466
4. Ceylan S, Koc K, Anik I (2010) Endoscopic endonasal transsphenoidal approach for pituitary adenomas invading the cavernous sinus. J Neurosurg 112:99–107. https://doi.org/10.3171/2009.4.JNS09182
5. Ciric I, Ragin A, Baumgartner C, Pierce D (1997) Complications of transsphenoidal surgery: results of a national survey, review of the literature, and personal experience. Neurosurgery 40:225–236 discussion 236-227
6. Cusimano MD, Fenton RS (1996) The technique for endoscopic pituitary tumor removal. Neurosurg Focus 1:e1 discussion 1p following e3
7. d'Avella E, Volpin F, Manara R, Scienza R, Della Puppa A (2013) Indocyanine green videoangiography (ICGV)-guided surgery of parasagittal meningiomas occluding the superior sagittal sinus (SSS). Acta Neurochir 155:415–420. https://doi.org/10.1007/s00701-012-1617-5
8. Dashti R, Laakso A, Niemela M, Porras M, Hernesniemi J (2009) Microscope-integrated near-infrared indocyanine green videoangiography during surgery of intracranial aneurysms: the Helsinki experience. Surg Neurol 71:543–550; discussion 550. https://doi.org/10.1016/j.surneu.2009.01.027

9. Dehdashti AR, Ganna A, Karabatsou K, Gentili F (2008) Pure endoscopic endonasal approach for pituitary adenomas: early surgical results in 200 patients and comparison with previous microsurgical series. Neurosurgery 62:1006–1015; discussion 1015-1007. https://doi.org/10.1227/01.neu.0000325862.83961.12
10. Ferroli P, Acerbi F, Albanese E, Tringali G, Broggi M, Franzini A, Broggi G (2011) Application of intraoperative indocyanine green angiography for CNS tumors: results on the first 100 cases. Acta Neurochir Suppl 109:251–257. https://doi.org/10.1007/978-3-211-99651-5_40
11. Ferroli P, Acerbi F, Broggi M, Broggi G (2013) The role of indocyanine green videoangiography (ICGV) in surgery of parasagittal meningiomas. Acta Neurochir 155:1035. https://doi.org/10.1007/s00701-013-1722-0
12. Ferroli P, Acerbi F, Tringali G, Albanese E, Broggi M, Franzini A, Broggi G (2011) Venous sacrifice in neurosurgery: new insights from venous indocyanine green videoangiography. J Neurosurg 115:18–23. https://doi.org/10.3171/2011.3.JNS10620
13. Fujisawa I, Asato R, Kawata M, Sano Y, Nakao K, Yamada T, Imura H, Naito Y, Hoshino K, Noma S et al (1989) Hyperintense signal of the posterior pituitary on T1-weighted MR images: an experimental study. J Comput Assist Tomogr 13:371–377
14. Gorczyca W, Hardy J (1988) Microadenomas of the human pituitary and their vascularization. Neurosurgery 22:1–6
15. Hide T, Yano S, Kuratsu J (2014) Indocyanine green fluorescence endoscopy at endonasal transsphenoidal surgery for an intracavernous sinus dermoid cyst: case report. Neurol Med Chir (Tokyo) 54:999–1003
16. Hide T, Yano S, Shinojima N, Kuratsu J (2015) Usefulness of the indocyanine green fluorescence endoscope in endonasal transsphenoidal surgery. J Neurosurg 122:1185–1192. https://doi.org/10.3171/2014.9.JNS14599
17. Hofstetter CP, Shin BJ, Mubita L, Huang C, Anand VK, Boockvar JA, Schwartz TH (2011) Endoscopic endonasal transsphenoidal surgery for functional pituitary adenomas. Neurosurg Focus 30:E10. https://doi.org/10.3171/2011.1.FOCUS10317
18. Holm C, Dornseifer U, Sturtz G, Ninkovic M (2010) Sensitivity and specificity of ICG angiography in free flap reexploration. J Reconstr Microsurg 26:311–316. https://doi.org/10.1055/s-0030-1249314
19. Holm C, Tegeler J, Mayr M, Becker A, Pfeiffer UJ, Muhlbauer W (2002) Monitoring free flaps using laser-induced fluorescence of indocyanine green: a preliminary experience. Microsurgery 22:278–287. https://doi.org/10.1002/micr.10052
20. Ito S, Muguruma N, Kimura T, Yano H, Imoto Y, Okamoto K, Kaji M, Sano S, Nagao Y (2006) Principle and clinical usefulness of the infrared fluorescence endoscopy. J Med Investig 53:1–8
21. Kawamata T, Amano K, Hori T (2008) Novel flexible forceps for endoscopic transsphenoidal resection of pituitary tumors: technical report. Neurosurg Rev 31:65–68; discussion 68. https://doi.org/10.1007/s10143-007-0108-2
22. Kim DL, Cohen-Gadol AA (2013) Indocyanine-green videoangiogram to assess collateral circulation before arterial sacrifice for management of complex vascular and neoplastic lesions: technical note. World Neurosurg 79(404):e401–e406. https://doi.org/10.1016/j.wneu.2012.07.028
23. Kim EH, Cho JM, Chang JH, Kim SH, Lee KS (2011) Application of intraoperative indocyanine green videoangiography to brain tumor surgery. Acta Neurochir 153:1487–1495; discussion 1494-1485. https://doi.org/10.1007/s00701-011-1046-x
24. Kimura T, Muguruma N, Ito S, Okamura S, Imoto Y, Miyamoto H, Kaji M, Kudo E (2007) Infrared fluorescence endoscopy for the diagnosis of superficial gastric tumors. Gastrointest Endosc 66:37–43. https://doi.org/10.1016/j.gie.2007.01.009
25. Kuroda K, Kinouchi H, Kanemaru K, Wakai T, Senbokuya N, Horikoshi T (2011) Indocyanine green videoangiography to detect aneurysm and related vascular structures buried in subarachnoid clots. J Neurosurg 114:1054–1056. https://doi.org/10.3171/2010.11.JNS1036
26. Kurokawa H, Fujisawa I, Nakano Y, Kimura H, Akagi K, Ikeda K, Uokawa K, Tanaka Y (1998) Posterior lobe of the pituitary gland: correlation between signal intensity on T1-weighted MR images and vasopressin concentration. Radiology 207:79–83. https://doi.org/10.1148/radiology.207.1.9530302
27. Litvack ZN, Zada G, Laws ER Jr (2012) Indocyanine green fluorescence endoscopy for visual differentiation of pituitary tumor from surrounding structures. J Neurosurg 116:935–941. https://doi.org/10.3171/2012.1.JNS11601
28. McLaughlin N, Eisenberg AA, Cohan P, Chaloner CB, Kelly DF (2013) Value of endoscopy for maximizing tumor removal in endonasal transsphenoidal pituitary adenoma surgery. J Neurosurg 118:613–620. https://doi.org/10.3171/2012.11.JNS112020
29. Mielke D, Malinova V, Rohde V (2014) Comparison of intraoperative microscopic and endoscopic ICG angiography in aneurysm surgery. Neurosurgery 10(Suppl 3):418–425; discussion 425. https://doi.org/10.1227/NEU.0000000000000345
30. Miki Y, Matsuo M, Nishizawa S, Kuroda Y, Keyaki A, Makita Y, Kawamura J (1990) Pituitary adenomas and normal pituitary tissue: enhancement patterns on gadopentetate-enhanced MR imaging. Radiology 177:35–38. https://doi.org/10.1148/radiology.177.1.2399335
31. Murakami K, Endo T, Tominaga T (2012) An analysis of flow dynamics in cerebral cavernous malformation and orbital cavernous angioma using indocyanine green videoangiography. Acta Neurochir 154:1169–1175. https://doi.org/10.1007/s00701-012-1354-9
32. Nishiyama Y, Kinouchi H, Senbokuya N, Kato T, Kanemaru K, Yoshioka H, Horikoshi T (2012) Endoscopic indocyanine green video angiography in aneurysm surgery: an innovative method for intraoperative assessment of blood flow in vasculature hidden from microscopic view. J Neurosurg 117:302–308. https://doi.org/10.3171/2012.5.JNS112300
33. Noura S, Ohue M, Seki Y, Tanaka K, Motoori M, Kishi K, Miyashiro I, Ohigashi H, Yano M, Ishikawa O, Miyamoto Y (2010) Feasibility of a lateral region sentinel node biopsy of lower rectal cancer guided by indocyanine green using a near-infrared camera system. Ann Surg Oncol 17:144–151. https://doi.org/10.1245/s10434-009-0711-2
34. Otani R, Fukuhara N, Ochi T, Oyama K, Yamada S (2012) Rapid growth hormone measurement during transsphenoidal surgery: analysis of 252 acromegalic patients. Neurol Med Chir (Tokyo) 52:558–562
35. Raabe A, Beck J, Gerlach R, Zimmermann M, Seifert V (2003) Near-infrared indocyanine green video angiography: a new method for intraoperative assessment of vascular flow. Neurosurgery 52:132–139 discussion 139
36. Raabe A, Nakaji P, Beck J, Kim LJ, Hsu FP, Kamerman JD, Seifert V, Spetzler RF (2005) Prospective evaluation of surgical microscope-integrated intraoperative near-infrared indocyanine green videoangiography during aneurysm surgery. J Neurosurg 103:982–989. https://doi.org/10.3171/jns.2005.103.6.0982
37. Sandow N, Klene W, Elbelt U, Strasburger CJ, Vajkoczy P (2015) Intraoperative indocyanine green videoangiography for identification of pituitary adenomas using a microscopic transsphenoidal approach. Pituitary 18:613–620. https://doi.org/10.1007/s11102-014-0620-7
38. Takagi Y, Kikuta K, Nozaki K, Sawamura K, Hashimoto N (2007) Detection of a residual nidus by surgical microscope-integrated intraoperative near-infrared indocyanine green videoangiography in a child with a cerebral arteriovenous malformation. J Neurosurg 107:416–418. https://doi.org/10.3171/PED-07/11/416
39. Tamura Y, Hirota Y, Miyata S, Yamada Y, Tucker A, Kuroiwa T (2012) The use of intraoperative near-infrared indocyanine green videoangiography in the microscopic resection of hemangioblastomas. Acta Neurochir 154:1407–1412; discussion 1412. https://doi.org/10.1007/s00701-012-1421-2

40. Tsuzuki S, Aihara Y, Eguchi S, Amano K, Kawamata T, Okada Y (2014) Application of indocyanine green (ICG) fluorescence for endoscopic biopsy of intraventricular tumors. Childs Nerv Syst 30:723–726. https://doi.org/10.1007/s00381-013-2266-6
41. Ueba T, Abe H, Matsumoto J, Higashi T, Inoue T (2012) Efficacy of indocyanine green videography and real-time evaluation by FLOW 800 in the resection of a spinal cord hemangioblastoma in a child: case report. J Neurosurg Pediatr 9:428–431. https://doi.org/10.3171/2011.12.PEDS11286
42. Ueba T, Okawa M, Abe H, Nonaka M, Iwaasa M, Higashi T, Inoue T, Takano K (2013) Identification of venous sinus, tumor location, and pial supply during meningioma surgery by transdural indocyanine green videography. J Neurosurg 118:632–636. https://doi.org/10.3171/2012.11.JNS121113
43. Woitzik J, Horn P, Vajkoczy P, Schmiedek P (2005) Intraoperative control of extracranial-intracranial bypass patency by near-infrared indocyanine green videoangiography. J Neurosurg 102:692–698. https://doi.org/10.3171/jns.2005.102.4.0692
44. Yamada S, Takada K (2003) Angiogenesis in pituitary adenomas. Microsc Res Tech 60:236–243. https://doi.org/10.1002/jemt.10262
45. Yamamoto Y, Shibuya H, Okunaka T, Aizawa K, Kato H (1999) Fibrin plugging as a cause of microcirculatory occlusion during photodynamic therapy. Lasers Med Sci 14:129–135. https://doi.org/10.1007/s101030050034
46. Zada G, Cavallo LM, Esposito F, Fernandez-Jimenez JC, Tasiou A, De Angelis M, Cafiero T, Cappabianca P, Laws ER (2010) Transsphenoidal surgery in patients with acromegaly: operative strategies for overcoming technically challenging anatomical variations. Neurosurg Focus 29:E8. https://doi.org/10.3171/2010.8.FOCUS10156